Biophysical Characterization and Management Effects on Semiarid Rangeland Observed From Landsat ETM+ Data

Hongliang Fang, Shunlin Liang, *Senior Member, IEEE*, Mitchel P. McClaran, Willem J. D. van Leeuwen, Sam Drake, Stuart E. Marsh, Allison M. Thomson, Roberto Cesar Izaurralde, and Norman J. Rosenberg

***Abstract*—Semiarid rangelands are very sensitive to global climatic change; studies of their biophysical attributes are crucial to understanding the dynamics of rangeland ecosystems under human disturbance. In the Santa Rita Experimental Range, AZ, the vegetation has changed considerably, and there have been many management activities applied. This study calculates seven surface variables: the enhanced vegetation index, the normalized difference vegetation index (NDVI), surface albedos (total shortwave, visible, and near-infrared), leaf area index (LAI), and the fraction of photosynthetically active radiation (FPAR) absorbed by green vegetation from the Enhanced Thematic Mapper (ETM+) data. Comparison with the Moderate Resolution Imaging Spectroradiometer vegetation index and albedo products indicates they agree well with our estimates from ETM+, while their LAI and FPAR are larger than from ETM+. Human disturbance has significantly changed the cover types and biophysical conditions. Statistical tests indicate that surface albedos increased and FPAR decreased following tree-cutting disturbances. The recovery will require more than 67 years and is about 50% complete within 40 years at the higher elevation. Grass cover, vegetation indexes, albedos, and LAI recovered from cutting faster at the higher elevation. Woody plants, vegetation indexes, and LAI have recovered to their original characteristics after 65 years at the lower elevation. More studies are needed to examine the spectral characteristics of different ground components.**

***Index Terms*—Albedo, Enhanced Thematic Mapper (ETM+), fraction of photosynthetically active radiation (FPAR), leaf area index (LAI), Moderate Resolution Imaging Spectroradiometer (MODIS), rangeland, remote sensing.**

I. INTRODUCTION

ARID and semiarid rangelands, covering 30% of the world's total land area [1], are very important for understanding terrestrial carbon dynamics. Studies have been carried out to examine regional carbon dynamics arising from human disturbance such as land use and management practices [2]. Yet, more studies are needed to improve our understanding of such issues as: 1) whether past management caused any difference to the rangeland; 2) whether and how local human disturbance will affect regional carbon dynamics; and 3) whether natural influence is positive or negative to the primary production.

The Santa Rita Experimental Range (SRER) (see descriptions about the study area in next section), located in south Arizona, is biogeographically typical of a large swath of semiarid rangelands [3]. Numerous studies have focused on soil and ecological development in SRER during the past century. Recently, research has been carried out to assess the human influence of carbon dynamics at the regional level by the authors. In particular, we were interested in determining the biophysical characteristics under different management practices, which are indispensable for understanding the carbon dynamics. Seven commonly used metrics were selected to study the biophysical characteristics of the rangeland: the enhanced vegetation index (EVI) and the normalized difference vegetation index (NDVI), surface broadband albedo, leaf area index (LAI), and the fraction of photosynthetically active radiation (FPAR) absorbed by the green vegetation.

Studies have been carried out to estimate these biophysical variables, especially with respect to areas with changing land management activities [4], [5]. For example, optical properties of overgrazing and protected areas were derived and compared [6]. Calculation of vegetation indexes is straightforward, and efforts have been made to derive surface albedos accurately [7]. Conventionally, LAI and FPAR are estimated through correlations with spectral vegetation indexes [8] or through the inversion of radiative transfer (RT) models [9]. However, reliable estimation of LAI and FPAR for semiarid rangeland is complicated because of the spectral mixture of canopy, litter, and ground [10], [11]. Gobron *et al.* [12] estimated FPAR with optimized vegetation indexes developed through RT simulation; however, these vegetation indexes are complicated in formation. Therefore, new methods are needed for this purpose.

The primary objective of this paper is to evaluate how different management practices will affect the land surface biophysical properties in SRER. To achieve that, we executed two tasks, first estimating surface biophysical variables from remotely sensed data, and then making a comparison of them between disturbed and control plots. A new LAI and FPAR estimation method was developed in this paper. After these parameters were estimated from Enhanced Thematic Mapper Plus (ETM+) data, they were compared with the Moderate Resolution Imaging Spectroradiometer (MODIS) standard products [13]. Statistical tests were conducted to evaluate

Manuscript received January 22, 2004; revised September 8, 2004. This work was supported in part by the National Aeronautics and Space Administration.

H. Fang and S. Liang are with the Department of Geography, University of Maryland, College Park, MD 20742 USA.

M. P. McClaran is with the School of Natural Resources, University of Arizona, Tucson, AZ 85719 USA.

W. J. D. van Leeuwen, S. Drake, and S. E. Marsh are with the Office of Arid Lands Studies, University of Arizona, Tucson, AZ 85719 USA.

A. M. Thomson, R. C. Izaurralde, and N. J. Rosenberg are with the Joint Global Change Research Institute, University of Maryland, College Park, MD 20742 USA.

Digital Object Identifier 10.1109/TGRS.2004.839813

whether different management practices have caused any significant change. Land cover characteristics were also analyzed since they were closely related to the optical and biophysical properties of the study area.

II. Study Area

The Santa Rita Experimental Range, founded in 1903, is located south of Tucson, AZ (31.8° N, 111.9° W). It has been a principal site for pioneer range research on the improvement and management of semiarid grasslands in the southwest U.S. [3]. It is characterized by long, gently sloping alluvial fans. Elevation ranges from 900–1400 m, and average annual precipitation increases from 275–450 mm along this gradient. The vegetation is currently a mixture of trees, shrubs, cacti and perennial grasses. Velvet mesquite (*Prosopis velutina*) is the most common species, and burroweed (*Isocoma tenuisecta*), cholla, and prickly pear (*Opuntia* spp.), and grama grass (*Bouteloua* spp.) and lovegrass (*Eragrostis lehmanniana*) are common shrub, cacti, and grass species, respectively [14]. In general, vegetation structure ranges from desert scrub at low elevations to mesquite-grass savanna at higher elevations.

Over the past century, the vegetation has changed considerably, and there have been many management activities applied to reverse those changes. Specifically, velvet mesquite has increased from $<1\%$ cover to $\sim$30% to 40% cover in many upland areas since 1900 [14]. In response to increasing velvet mesquite, several projects of tree removal were applied between 1930 and 1980. Mesquite removals performed in the 1930s and 1960s provide areas for comparison with locations where mesquite has been allowed to increase unabated.

Six study sites were selected to represent three types of settings [Fig. 1(a)]: where all mesquite trees were cut and killed in 1935 and 1937 (C_1935 and E_1937); where about half of all trees were killed [15] with aerially applied herbicide in the early 1960s (D_1960 and D_1962); and control sites where the mesquite increase was not reversed (D_control and E_control). All sites are in two general locations: the upper elevation at approximately 1100 m including C_1935, D_1960, D_1962, and D_control; and the lower elevation at approximately 1000 m including E_1937 and E_control. Study sites C and D are within 1 km of each other, and study sites E are adjacent to each other. The size of each site ranges from 4–6 ha. D_control serves as an untreated comparison for the nearby C_1935, D_1960, and D_1962.

The C_1935 and E_1937 sites are some of the oldest mesquite-killed areas on the study area, and they serve to help estimate how long the clearing effort would last before the sites would return to uncut conditions. The D_1960 and D_1962 sites serve as intermediate-aged mesquite-killed areas and therefore serve the same role for estimating the longevity of the treatment. The two elevations provide the opportunity to compare the rates of recovery following tree removal in relation to elevation.

III. Methods

Using Landsat ETM+ data to estimate the surface biophysical variables, the initial step was to convert radiance recorded at the top of the atmosphere to surface reflectance using an atmospheric correction algorithm [16]. Vegetation indexes and all other variables were calculated from ETM+surface reflectance and then compared with MODIS standard products.

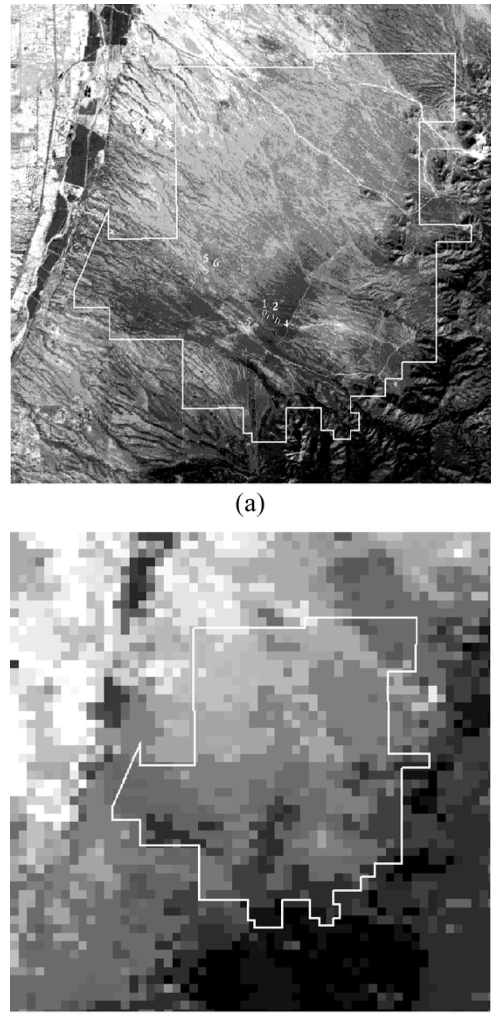

(a)

(b)

Fig. 1. (a) Landsat ETM+ standard (grayscale) composite image of the Santa Rita Experimental Range (SRER) on September 25, 2002. The small color boxes are six study plots (1, C_1935; 2, D_1960; 3, D_1962; 4, D_control; 5, E_1937; 6, E_control). (b) MODIS surface reflectance (MOD09) image of the same area (RGB: 214) on the same day. The SRER is delineated with white lines.

A. Vegetation Index and Albedo Calculation

NDVI is calculated by

$$\mathrm{NDVI} = \frac{\rho_{\mathrm{NIR}} - \rho_R}{\rho_{\mathrm{NIR}} + \rho_R} \tag{1}$$

where ρ_R and ρ_{NIR} are surface reflectance at red and near infrared (NIR), respectively. EVI optimizes the vegetation signal and reduces the background and atmospheric influence. EVI is defined by

$$\mathrm{EVI} = \frac{G(\rho_{\mathrm{NIR}} - \rho_R)}{\rho_{\mathrm{NIR}} + C_1\rho_R - C_2\rho_B + L} \tag{2}$$

where ρ_B is the blue band reflectance, L is the canopy background adjustment, and C_1 and C_2 are the coefficients of the aerosol resistance term. The coefficients used in the EVI algorithm are $L = 1$, $C_1 = 6$, $C_2 = 7.5$, and G (gain factor) $= 2.5$ [17].

Surface broadband albedos are computed by the following equations [18]:

$$\begin{aligned}\alpha_{\mathrm{SW}} &= 0.356\alpha_1 + 0.130\alpha_3 + 0.373\alpha_4 + 0.085\alpha_5 \\ &\quad + 0.072\alpha_7 - 0.0018 \\ \alpha_{\mathrm{VIS}} &= 0.443\alpha_1 + 0.317\alpha_2 + 0.240\alpha_3 \\ \alpha_{\mathrm{NIR}} &= 0.693\alpha_4 + 0.212\alpha_5 + 0.116\alpha_7 - 0.003 \end{aligned} \tag{3}$$

where α_{SW}, α_{VIS}, and α_{NIR} are the total shortwave, total visible, and total NIR albedo, respectively, and α_i is the spectral albedo of each ETM+ band. If the surface is assumed to be Lambertian, the spherical albedos are numerically equivalent to spectral reflectances from atmospheric correction.

B. Surface LAI Estimation

In this paper, a new hybrid approach was developed to estimate LAI and FPAR. The new approach extends from a previous study estimating crop LAI from ETM+ data [19]. The essential idea is to estimate LAI with a neural network method based on simulated databases. In the radiative transfer simulation, soil reflectances are derived from the instant remotely sensed images. Major steps of this approach are as follows:

- perform atmospheric correction of the ETM+ image to obtain surface reflectance;
- identify soil pixels and estimate the soil reflectance index (SRI) from the red and NIR reflectance scatterplot;
- construct a database through a canopy radiative transfer model (e.g., the MCRM model by [20]) simulation with a variety of input parameters;
- train a neural network with the simulated database;
- predict the surface LAI with the training results.

LAI can be estimated from the atmospherically corrected surface reflectances as well as top of atmospheric (TOA) radiance data. Atmospherically corrected ETM+ band 3 and 4 are most appropriate in LAI estimation. The method has been validated and works well for both Landsat ETM+ and EO1 ALI data [21].

C. Surface FPAR Estimation

We extended the hybrid LAI estimation algorithm [19] to estimate surface FPAR. The approach integrated the conventional RT inversion method and neural network method. In the neural network training process, FPAR was in the input layer. The output layer consisted of the simulated six ETM+ bands. In the prediction process, the atmospherically corrected ETM+ reflectances were used to estimate FPAR. Different kinds of band combinations were tested, and all three visible bands (band 1, 2, and 3) were used since they have the most stable outputs.

FPAR is computed by [22]

$$\mathrm{FPAR} = 1 - \alpha - A_g \tag{4}$$

where α is the surface albedo and A_g is the absorptance of the soil. For a Lambertian surface, the value of α is equal to the nadir reflectance observed by ETM+. A_g can be calculated by

$$A_g = A_0 + A_d \tag{5}$$

where A_0 and A_d are the absorbed direct (single scattering) and diffuse (multiple scattering) radiance, respectively. The soil absorptance is given by the following equations:

$$A_0 = S_0 * q_0 * (1 - R_{s0}) \tag{6}$$

where S_0 is the portion of single-scattering illumination, q_0 the canopy transmittance of direct radiation, and R_{s0} the bidirectional reflectance of soil; and

$$A_d = (S_0 * t_0 + S_d * t_d) * (1 - R_{sd}) \tag{7}$$

where t_0 and t_d are canopy diffuse transmittance for direct and diffuse incoming radiation, respectively, S_d the portion of skylight, and R_{sd} the bihemispheric soil reflectance.

The simulated reflectances from Section III-B were used to construct the database for FPAR training. Obviously, a common database can be used for both LAI and FPAR estimation. Values obtained for α and A_g were integrated over all visible bands to obtain the surface albedo and soil absorptance over 400–700 nm.

D. Statistical Analysis

After the biophysical variables were derived, their values for the treatment sites and the control sites were compared statistically to see if the management measures have caused any significant difference. The treatment sites and control sites are assumed independent from each other and there is mutual independence between any pair of samples. In this case, the Wilcoxon rank sum W test, a nonparametric alternative to the difference or means test, is appropriate [23]. It is useful for analyzing differences between two samples and making inferences to corresponding populations. The hypotheses of two sample Wilcoxon W tests are as follows:

- H_0: Distribution of measurements for the first population is equal to that of the second population.
- H_A: Distribution of measurements for the first population is larger (or smaller) than that for the second population (one-tailed).

The test statistic is

$$Z_w = \frac{W_i - \overline{W_i}}{s_w} \tag{8}$$

where W_i is the sum of ranks of sample i, and $\overline{W_i}$ and s_w represent the theoretical mean and standard deviation of W_i, respectively.

Given the settings of the study area, we performed four groups of Wilcoxon tests among study sites: 1) comparing sites at upper elevation (sites C_1935, D_1960, D_1962, and D_control); 2) comparing sites at lower elevation (E_1937 and E_control); 3) comparing the difference among upper sites and

TABLE I
MODIS DATA USED IN THE STUDY. THESE DATA WERE OBTAINED FROM THE NATIONAL AERONAUTICS AND SPACE ADMINISTRATION EARTH OBSERVING SYSTEM DATA GATEWAY

MODIS data	Product number	Resolution (m)	Julian day	Note
Surface reflectance	MOD09GHK	500	268	(daily)
Albedo	MOD43B3	1000	257	(16 day)
Vegetation index	MOD13A1	500	257	(16 day)
LAI and FPAR	MOD15A2	1000	265	(8 day)
NPP	MOD17A3	1000	Year 2001	(whole year)

the differences among lower sites to compare the vegetation recovery speed at two elevations; and 4) comparing the difference between upper and lower sites.

IV. REMOTE SENSING AND FIELD DATA COLLECTION

The Landsat ETM+ image was acquired on September 25, 2002, when it was clear and cloudless (Fig. 1). The solar zenith angle (SZA) was 39.11°, and the azimuth angle was 142.02°. The ETM+ data were registered to UTM coordinates (Zone 12). Atmospheric correction of the ETM+ was performed to obtain the surface reflectance [16]. It is noted the SRER is not homoegeneous at the ETM+ pixel scale [Fig. 1(a)]. Some linear ditches are obvious in the ETM+ images, although they occupy only a small portion of the plot. Those pixels are treated as an integrated phenomenon of the grassland.

The MODIS vegetation index, albedo, LAI, and FPAR products were obtained by using the gateway at Earth Resources Observation System (EROS) Data Center (EDC) (Table I). A composite image of MODIS surface reflectance is shown in Fig. 1(b). The MODIS data were projected to the same projection as the ETM+ data (UTM 12) and then resampled to 500-m resolution with the MODIS Reprojection Tool (MRT).

A five-day field campaign was carried out from September 23–27, 2002 during the satellite overpass. Land cover types of tree, shrub, grass, and bare ground were estimated for each study site during the field campaign. In each area, a point intercept technique [24] was used to estimate cover along ten randomly located transects consisting of 100 points each for a total of 1000 points for each site. All layers of vegetation were recorded; and, therefore when the cover sums to $>100\%$, it reflects that some shorter shrubs or grass are found under the taller trees or shrubs.

Surface reflectance was measured with the Analytical Spectral Devices (ASD) [25]. ASD measures the reflectance over 350–2500 nm wavelengths. At each plot, more than 100 random measurements were taken. The average reflectance is used to represent total plot reflectance. Some researchers measure different surface components, such as bare sands, biological soil crusts, annuals, and perennials for spectral unmixing analysis [11]. With this method, the plot reflectance is obtained from a spectral composition based on coherent land cover measurement. However, annuals or perennials are often affected by background soil within the ASDs field of view (FOV), and it is nearly impossible to get a pure component within the FOV.

Field LAI was measured for E_1937 and E_control with LAI-2000 Plant Canopy Analyzer in the 2002 campaign. Unfortunately, field measurement was very difficult in such discontinuous plant communities. In October 2003, we did a second field campaign. AccuPAR linear PAR ceptometer was used to take field LAI and FPAR measurements. AccuPAR is advantageous because it does not require the diffuse radiation conditions. The operation procedures were carefully followed in order to minimize system errors. Some mature forest sites near SRER were measured. We assume that the LAI and FPAR measures are comparable with a year ago.

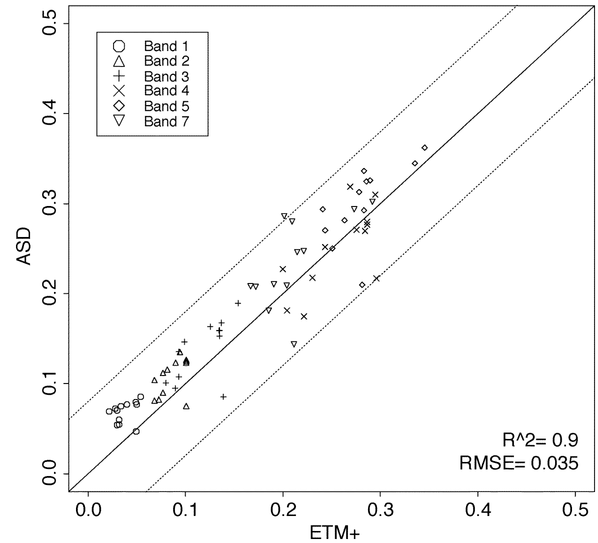

Fig. 2. Comparison of the retrieved ETM+ reflectance and the aggregated ASD measured reflectance. The two dashed lines represent ± 0.08 away from the solid 1 : 1 line.

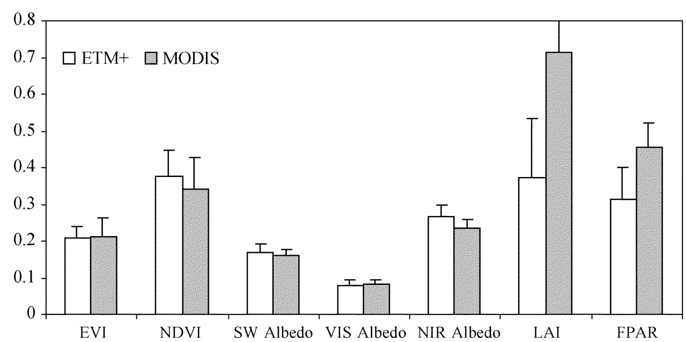

Fig. 3. Comparison of the biophysical attributes derived from ETM+ and MODIS. The mean values and the standard deviation (in error bars) are shown.

V. RESULTS

With the help of MODTRAN, atmospheric correction was performed with a desert atmospheric profile and a default visibility of 40 km. Nearly all of the retrieved ETM+ reflectances are within $\pm 8\%$, and most pixels (74%) are within $\pm 5\%$ off the field measured values (Fig. 2). The root mean square errors (RMSE) between the ETM+ reflectances and the aggregated ASD reflectances are as low as 0.035 (Fig. 2). Although some points do not match perfectly, given the surface heterogeneity in the study sites and uncertainties of the field measurements, this result is notably accurate and was used in the following analyses.

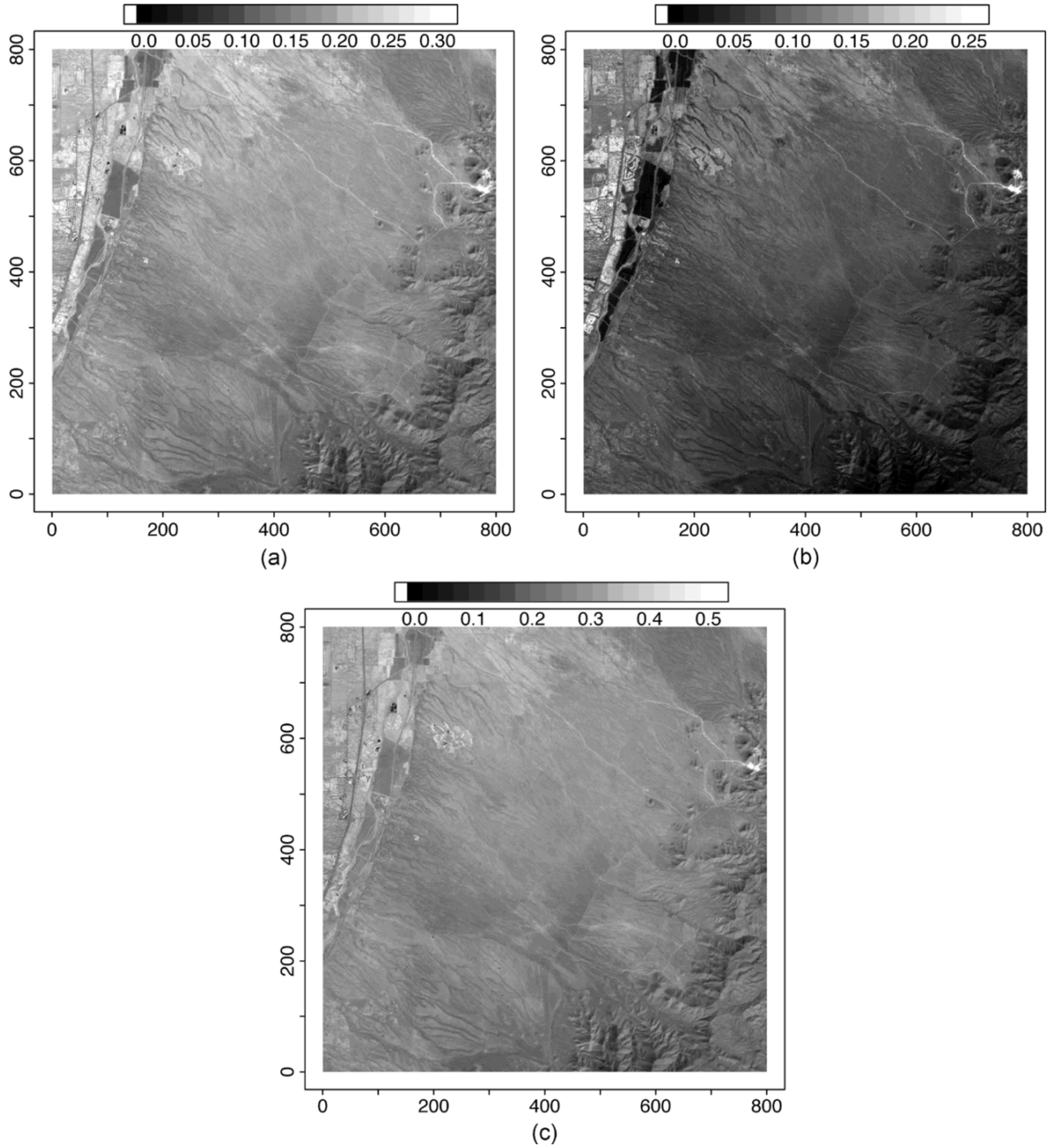

Fig. 4. Land surface broadband albedo maps estimated with the hybrid approach. (a) Total shortwave. (b) Total visible. (c) Total NIR.

A. *Biophysical Characteristics of SRER*

All seven biophysical parameters were calculated successfully with the method in Section III and were compared with equivalent MODIS products (Fig. 3). NDVI and EVI maps were calculated with (1) and (2), respectively. For brevity, these maps are not shown, but their values were examined in the statistical analysis. There is a very good fit between the ETM+ and MODIS vegetation index (Fig. 3). The MODIS EVI value is lower than the NDVI product. So are the ETM+ products. The minor differences between the MODIS and ETM+ vegetation index products are mainly caused by the scale difference. The SRER is very homogeneous in the MODIS image, but not at ETM+ resolution. MODIS LAI and FPAR products are higher than our estimation from ETM+ (Fig. 3).

The broadband albedo maps (Fig. 4) were derived with equations in (3). In SRER, the total shortwave albedo ranges from 0.063–0.329. In fact, only three pixels' shortwave albedos are larger than 0.3. The minimum and maximum albedos are 0.01 and 0.247 for the visible band and 0.106 and 0.424 for the NIR band, respectively. The ETM+ albedo results are very similar to the MODIS albedo products (Fig. 3). The maximum difference (0.027) is observed for the total NIR albedo. This is attributed to the resolution difference between ETM+ and MODIS. To verify the accuracy of the converted broadband albedo products, they are compared with albedometer measurements in Fig. 5. The overall R^2 is 0.972, and the RMSE is less than 0.05. There are some differences in the near infrared bands. They are attributed mainly to the scale mismatch between point measurement and the 30-m ETM+ pixel. Surface heterogeneity and measurements limitations (only vegetation <2 m are measured) also contribute to the deviation.

LAI and FPAR derived from ETM+are smaller than those from MODIS (Fig. 3). This is mainly due to their different spa-

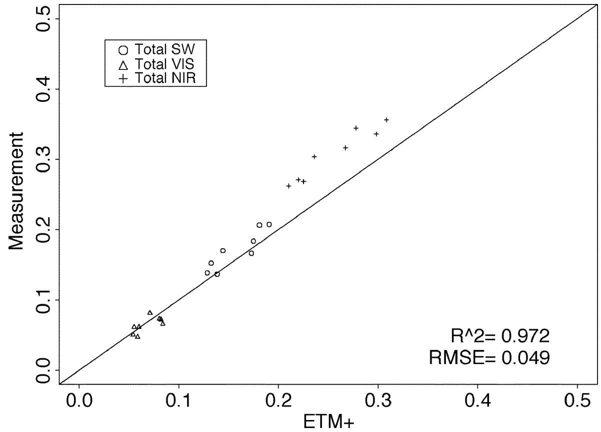

Fig. 5. Comparing the converted total shortwave, total visible, and total NIR albedos from ETM+ imagery with albedometer measurements.

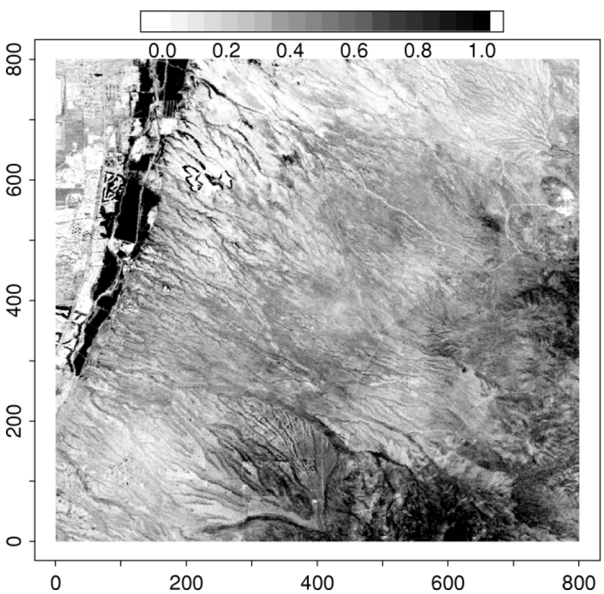

Fig. 6. LAI of the SRER estimated from the Landsat ETM+ (800 × 800). Values greater than 1.0 are shown with the grayscale index of 1.0 for better visual effect.

tial resolutions and algorithms: ETM+ revealed much of the spatial complexity of land cover at the sites (trees, shrubs, grasses, and bare ground); in contrast, there is only one type (shrub) in the MODIS LAI/FPAR algorithm's biome map. LAI and FPAR for the whole SRER region are shown in Figs. 6 and 7, respectively. Of all the LAI in this 800 × 800 region, over 96% are less than 1.0. In order to show the lower LAI pixels clearly, LAI values higher than 1.0 have been zipped to the highest value (1.0) in the legend bar. There are some forest stripes in the upper left corner of the figure whose LAI values are as high as 3.0–4.0. These forest strips are probably the pecan tree farms located at elevations below the Santa Rita. The forest LAI at the lower corner is around 0.5–2.0. In the SRER, most of the LAI values are around 0.3–0.6 (Fig. 6). The LAI distribution, typical of a sloping alluvial fan, shows higher values in the drainages than in the adjacent uplands. The distribution of the FPAR (Fig. 7) is quite similar to that of the LAI due to their similar physical characteristics. The forest FPAR can be above 0.8 and the grassland FPAR between 0.2 and 0.5 in the study area.

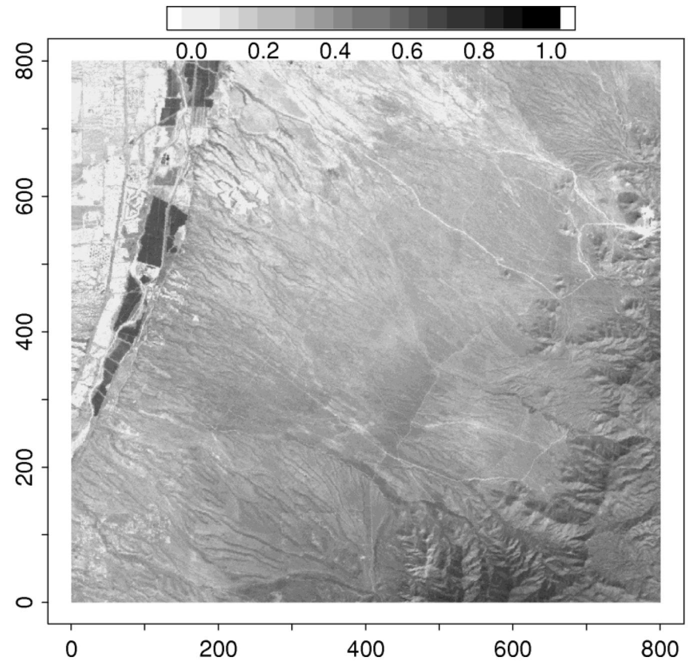

Fig. 7. FPAR of the SRER estimated from the Landsat ETM+ (800 × 800).

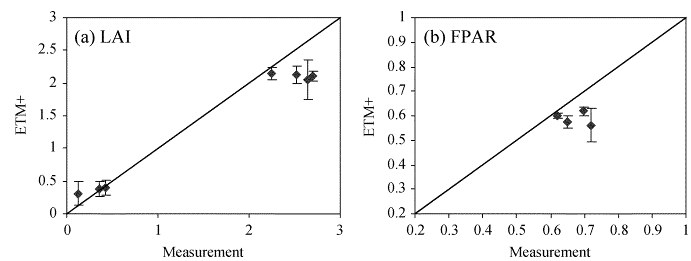

Fig. 8. Comparison of (a) LAI and (b) FPAR estimated from ETM+ with field measurements.

TABLE II
LAND COVER CHARACTERISTICS (PERCENT) OF THE STUDY SITES. "WOODY PLANTS" IS THE SUM OF TREE AND SHRUB COVER

Study Area	Tree	Shrub	Woody Plants	Grass	Bare Ground
C_1935	25.3	10.3	35.6	35.7	41.7
D_1960	15.7	7.4	23.1	44.4	41.6
D_1962	15.5	6.4	21.9	34.2	51.1
D_control	29.6	12.3	41.9	25.1	46.1
E_1937	13.4	18.7	32.1	17.0	56.7
E_control	17.9	16.7	34.6	24.4	50.6

Estimations of LAI and FPAR were compared with ground-measured values (Fig. 8). Results from a few forest and grass points demonstrate that LAI and FPAR estimated from ETM+ compared fairly well with field measurements. However, ETM+ estimation is lower than field measurements for both LAI and FPAR. This is understandable because the field measurements included the tree trunks and branches. Some studies take into account the leaf–plant ratio for such a woody plant environment [10], [26], which would make the results more accurate. More ground measurements are needed in this area.

B. Management Effects on Rangelands

The land cover characteristics for the study sites are shown in Table II. All trees and shrubs are combined into a woody

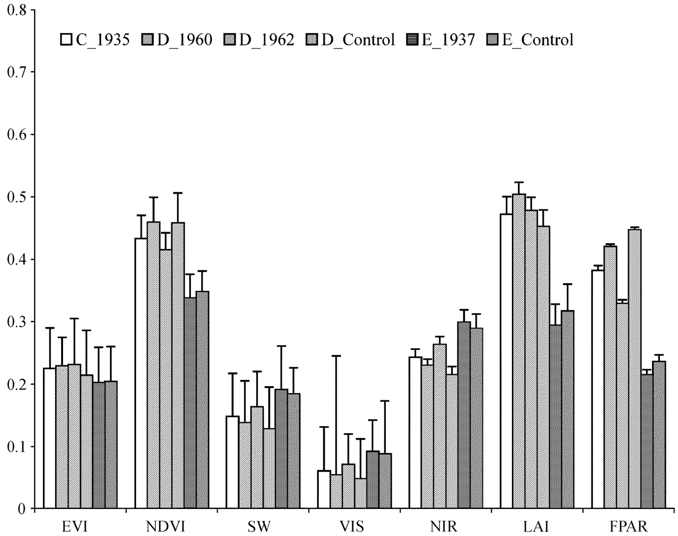

Fig. 9. Mean value and standard deviation (error bars) for EVI, NDVI, albedo, LAI, and FPAR for each plot.

plant category. The mean values of EVI, NDVI, albedo, LAI, and FPAR for each site are shown in Fig. 9. Wilcoxon test results are shown in Table III.

Comparing Sites at Upper Elevation (Sites C_1935, D_1960, D_1962, and D_control): Based on cover types, woody plant cover decreases from the uncut (D_control) to the oldest cut area (C_1935), and the lowest values are where the most recent mesquite treatment (herbicides) was applied (D_1960 and D_1962). This suggests that recovery will require more than 67 years, but it is more than 50% complete within 40 years. However, for grass cover there is a different pattern. Grass cover is least in the uncut situation, but there are no consistent differences among the areas where mesquite were killed at different times in the past.

EVI seems to show a negative relationship with the woody plant coverage and a positive relationship with grass coverage. EVI decreases from the oldest cut area (C_1935) to the uncut site (D_control), and the highest values are at the most recent treatment sites (D_1960 and D_1962). The NDVI of C_1935 and D_1962 have decreased after treatment. Artificial treatment significantly increased the surface total shortwave, visible, and NIR albedos for all sites. The LAI values of the treated sites are also significantly larger than those of the control sites due to the higher grass cover of the treated sites. However, FPAR values decrease after treatment. The albedo, LAI, and FPAR values are still not recovered after 67 years. Comparison among treatment sites is complicated. For example, the albedo values for D_1962 are higher than C_1935, which are higher than D_1960. Note that there is no difference between the NDVI of D_1960 and D_control, nor between the LAI of D_1962 and C_1935.

Comparing Sites at Lower Elevation (E_1937 and E_control): Based on the cover types, woody plant cover is not different between the two study sites, although tree cover is greater in the uncut site (E_control). This suggests that recovery of woody cover occurs within 65 years. But, the difference in tree cover may reflect a slow growth rate of trees at the lower elevation. For grass cover there is a similar pattern. Bare ground fraction is greater in the treated site. Corresponding to these cover type patterns, the surface albedos in E_1937 are significantly greater than in the uncut situation. There is a different pattern for FPAR. FPAR is higher in the control site. There is no significant difference for vegetation indexes and LAI at the lower elevation. They have recovered to their original characteristics after 65 years.

Comparing the Recovery Rates at Upper and Lower Elevations: At the lower elevation, the conditions are drier and warmer than at the higher elevation. Therefore, we would expect faster recovery from cutting at higher elevation and more bare ground at the lower elevation. As expected, Table III demonstrates that grass cover recovered from cutting faster at the higher elevation. The vegetation indexes, albedo estimates, and LAI exhibit the same pattern.

Comparing the Difference Between Upper and Lower Sites: Vegetation indexes, LAI, and FPAR increase with elevation, while albedo values decrease with elevation. This pattern corresponds well to the cover type. Tree cover and grass cover increase with elevation, and shrub cover is greater at lower elevation. These patterns are consistent with the expectation [14] of more mesquite-grassland vegetation at upper elevations versus desert scrub vegetation at lower elevations, which are dominated by shrub species (Table II).

VI. Summary and Conclusion

To evaluate the impacts of the management practice on biophysical properties of the semiarid rangeland in the SRER, a set of biophysical variables were estimated from ETM+ data. The data included vegetation indexes, surface broadband albedos, and LAI based on the existing algorithms, as well as FPAR calculated using a new method developed in this study. The Wilcoxon statistical test was used to evaluate the response of vegetation to management practices.

The average total shortwave, total visible, and total NIR albedo of SRER is 0.27, 0.17, and 0.08, respectively. The albedo data are very accurate compared with field measurements ($\mathrm{RMSE} < 0.05$). A hybrid approach, which integrated the advantages of convectional canopy radiative transfer simulation and nonparametric neural network methods, was developed to estimate LAI and FPAR from Landsat ETM+ data. For SRER, the LAI is between 0.3–0.6, and the FPAR between 0.2–0.5. The estimated LAI and FPAR values are very reasonable compared with ground measurements and other data sources.

Ultimately, the vegetation indexes, broadband albedos, LAI, and FPAR calculated from ETM+ were compared with the corresponding MODIS land surface products. The ETM+ and MODIS vegetation indexes are in agreement with each other. Their EVI values are lower than the NDVI products. MODIS albedo products matched very well with the ETM+ results, while LAI and FPAR overestimated. Different spatial scales between MODIS and ETM+ data may have contributed to the difference to some extent.

To study the human disturbance on canopy attributes, the treated and control sites were compared. The two elevations provide the opportunity to compare the magnitude of cover types. Comparison of cover types suggests that recovery will require more than 67 years, but it is more than 50% complete within

TABLE III
WILCOXON SIGNIFICANCE LEVEL FROM THE STATISTICAL COMPARISON OF TREE, BRUSH, WOOD, AND GRASS FRACTIONS, AND EVI, NDVI, ALBEDO, LAI, AND FPAR VALUES FOR DIFFERENT TREATMENT AND ELEVATIONS. "+" ("-") MEANS THE FIRST TREATMENT SITE(S) IS/ARE LARGER (OR LESS) THAN THE SECOND

	Tree	Shrub	Wood	Grass	EVI	NDVI	SW	VIS	NIR	LAI	FPAR
C35/D60	0.001	0.048	0.004	-0.173	-0.109	- (0)	+ (0)	+ (0)	+ (0)	-0.003	- (0)
C35/D62	0.008	0.014	0.001	0.515	-0.029	+ (0)	- (0)	- (0)	- (0)	-0.652	+ (0)
C35/DCon	-0.203	-0.203	-0.041	0.005	+ (0)	- (0)	+ (0)	+ (0)	+ (0)	0.018	- (0)
D60/D62	0.192	0.381	0.120	0.153	-0.279	+ (0)	- (0)	- (0)	- (0)	0.001	+ (0)
D60/DCon	- (0)	-0.017	- (0)	0.002	+ (0)	0.523	+ (0)	+ (0)	+ (0)	+ (0)	- (0)
D62/DCon	-0.001	-0.004	- (0)	0.001	+ (0)	- (0)	+ (0)	+ (0)	+ (0)	0.017	- (0)
E37/ECon	-0.070	0.113	-0.26	-0.038	-0.338	-0.113	+ (0)	0.014	+ (0)	-0.166	-0.015
DCon-D60/DCon-D62	-0.312	-0.455	-0.236	-0.236	0.682	- (0)	+ (0)	+ (0)	+ (0)	-0.002	- (0)
DCon-D60/ECon-E37	0.016	0.014	0.001	- (0)	- (0)	-0.068	-0.046	-0.253	-0.01	- (0)	0.423
DCon-D62/ECon-E37	0.003	0.007	+ (0)	- (0)	- (0)	+ (0)	- (0)	- (0)	- (0)	-0.015	+ (0)
High/Low	0.009	- (0)	-0.2137	+ (0)	+ (0)	+ (0)	- (0)	- (0)	- (0)	+ (0)	+ (0)

40 years at the higher elevation. Human disturbance has increased the surface total shortwave, visible, and NIR albedos at the higher elevation. LAI has increased after tree removal, while FPAR value decreased. The albedo, LAI and FPAR values may take more than 67 years to recover to their control site conditions. At the lower elevation, woody plant cover has recovered within 65 years. There is no difference for vegetation indexes and LAI in the treated site. However, surface albedos are still significantly greater and FPAR lower in the treated site.

Grass cover recovered faster from cutting at the higher elevation. As a result, the vegetation indexes, albedo estimates, and LAI recovered faster at the higher elevation. Vegetation indexes, LAI, and FPAR increase with elevation, and albedo values decrease with elevation, corresponding to the cover type. Tree cover and grass cover increases with elevation, and shrub cover is greater at lower elevation.

Studies in this paper are crucial to the understanding of carbon dynamics under different management practices. Carbon changes in management and natural ecosystems are driven largely by land use and management practices [2]. From the data provided in this paper, local carbon dynamics of primary production can be extracted. Data derived from high spatial resolution, remotely sensed data at landscape scales can by used in scaling-up local models to study the impact of local human disturbance on regional carbon dynamics. Our results also satisfy the requirement in managing large tracts of semiarid lands. In addition to the impact of human disturbance, it is also necessary to study the effects of natural processes (such as grass fires) to the canopy characteristics and local carbon dynamics in general.

ACKNOWLEDGMENT

The authors gratefully acknowledge C. Shuey, C.-Y. Huang, and K. Mandapaka, who participated in the field measurements, and A. Russ, who helped prepare the instrument.

REFERENCES

[1] J. F. Reynolds and D. M. S. Smith, "Do humans cause deserts?," in *Global Desertification: Do Humans Cause Deserts?*, J. F. Reynolds and D. M. S. Smith, Eds. Berlin, Germany: Dahlem Univ. Press, 2002, pp. 1–21.

[2] R. A. Houghton, J. L. Hackler, and K. T. Lawrence, "The U.S. carbon budget: Contribution from land-use change," *Science*, vol. 285, pp. 574–578, 1999.

[3] N. F. Sayre, "Recognizing history in range ecology: 100 years of science and management of the Santa Rita experimental range," in *Santa Rita Experimental Range: 100 years (1903 to 2003) of Accomplishments and Contributions*. Ogden, UT: U.S. Dept. Agriculture, Forest Service, Rocky Mountain Res. Station, 2003.

[4] J. R. G. Townshend, C. Justice, W. Li, C. Gurney, and J. McManus, "Global land cover classifiication by remote sensing: Present capabilities and future possibilities," *Remote Sens. Environ.*, vol. 35, pp. 243–255, 1991.

[5] S. W. Running, C. Justice, V. Salomonson, D. Hall, J. Barker, Y. J. Kaufman, A. Strahler, A. Huete, J. M. V. Vanderbilt, Z. Wan, P. Teillet, and D. Carneggie, "Terrestrial remote sensing science and algorithms planned for EOS/MODIS," *Int. J. Remote Sens.*, vol. 15, pp. 3587–3620, 1994.

[6] J. Otterman, A. Karnieli, T. Brakke, D. Koslowsky, H. J. Bolle, D. Starr, and H. Schmidt, "Desert scrub optical density and spectral-albedo ratios of impacted-to-protected areas by model inversion," *Int. J. Remote Sens.*, vol. 23, pp. 3959–3970, 2002.

[7] S. Liang, *Quantitative Remote Sensing of Land Surfaces*. New York: Wiley, 2003, p. 550.

[8] F. Baret and G. Guyot, "Potential and limits of vegetation indices for LAI and APAR assessment," *Remote Sens. Environ.*, vol. 35, pp. 161–173, 1991.

[9] Y. Knyazikhin, J. V. Martonchik, R. B. Myneni, D. J. Dine, and S. W. Running, "Synergistic algorithm for estimating vegetation canopy leaf area index and fraction of absorbed photosynthetically active radiation from MODIS and MISR data," *J. Geophys. Res.*, vol. 103, pp. 32 257–32 276, 1998.

[10] M. A. White, G. P. Asner, R. R. Nemani, J. L. Privette, and S. W. Running, "Measuring fractional cover and leaf area index in arid ecosystems: Digital camera, radiation transmittance, and laser altimetry methods," *Remote Sens. Environ.*, vol. 74, pp. 45–57, 2000.

[11] G. P. Asner and K. B. Heidebrecht, "Spectral unmixing of vegetation soil and dry carbon cover in arid regions: Comparing multispectral and hyperspectral observations," *Int. J. Remote Sens.*, vol. 23, pp. 3939–3958, 2002.

[12] N. Gobron, B. Pinty, M. M. Verstraete, and J. Widlowshi, "Advanced vegetation indices optimized for up-coming sensors: Design, performance, and applications," *IEEE Trans. Geosci. Remote Sens.*, vol. 38, no. 6, pp. 2489–2505, Nov. 2000.

[13] C. O. Justice, J. R. G. Townshend, E. F. Vermote, E. Masuoka, R. E. Wolfe, N. Saleous, D. P. Roy, and J. T. Morisette, "An overview of MODIS land data processing and product status," *Remote Sens. Environ.*, vol. 83, pp. 3–15, 2002.

[14] M. P. McClaran, "A century of vegetation change on the Santa Rita experimental Range," in *Santa Rita Experimental Range: 100 years (1903 to 2003) of Accomplishments and Contributions*. Ogden, UT: U.S. Dept. Agriculture, Forest Service, Rocky Mountain Res. Station, 2003, pp. 16–33.

[15] S. C. Martin and D. E. J. Ward, "Using aerial applications-two annual sprays control mesquite," *Progr. Agricult. Arizona*, vol. 18, pp. 20–21, 1966.

[16] S. Liang, H. Fang, and M. Chen, "Atmospheric correction of Landsat ETM+ land surface imagery: I. Methods," *IEEE Trans. Geosci. Remote Sens.*, vol. 39, no. 11, pp. 2490–2498, Nov. 2001.

[17] A. Huete, K. Didan, T. Miura, E. P. Rodriguez, X. Gao, and L. G. Ferreira, "Overview of the radiometric and biophysical performance of the MODIS vegetation indices," *Remote Sens. Environ.*, vol. 82, pp. 195–213, 2002.

[18] S. Liang, "Narrowband to broadband conversions of land surface albedo: I. Formulae," *Remote Sens. Environ.*, vol. 76, pp. 213–238, 2001.

[19] H. Fang and S. Liang, "Retrieve LAI from Landsat 7 ETM+ data with a neural network method: Simulation and validation study," *IEEE Trans. Geosci. Remote Sens.*, vol. 41, no. 9, pp. 2052–2062, Sep. 2003.

[20] A. Kuusk, "Monitoring of vegetation parameters on large areas by the inversion of a canopy reflectance model," *Int. J. Remote Sens.*, vol. 19, pp. 2893–2905, 1998.

[21] S. Liang, H. Fang, L. Thorp, M. Kaul, T. G. V. Niel, T. R. McVicar, J. Pearlman, C. Walthall, C. Daughtry, F. Huemmrich, and D. L. B. Jupp, "Estimation and validation of land surface broadband albedos and leaf area index from EO-1 ALI data," *IEEE Trans. Geosci. Remote Sens.*, vol. 41, no. 6, pp. 1260–1267, Jun. 2003.

[22] L. Moreau and Z. Li, "A new approach for remote sensing of canopy absorbed photosynthetically active radiation. II. Proportion of canopy absorption," *Remote Sens. Environ.t*, vol. 55, no. 3, pp. 192–204, 1996.

[23] J. C. McGrew and C. B. Monroe, *An Introduction to Statistical Problem Solving in Geography*. Dubuque, IA: Brown, 1993.

[24] R. A. Evans and R. M. Love, "The step-point method of sampling: A practical tool in range research," *J. Range Manage.*, vol. 10, pp. 208–212, 1957.

[25] ASD, *FieldSpec Pro User's Guide*. Boulder, CO: Analytical Spectral Devices, 2000.

[26] M. J. Chopping, A. Rango, K. M. Havstad, F. R. Schiebe, J. C. Ritchie, T. J. Schmugge, A. N. French, L. Su, L. McKee, and M. R. Davic, "Canopy attributes of desert grassland and transition communities derived from multiangular airborne imagery," *Remote Sens. Environ.*, vol. 85, pp. 339–354, 2003.

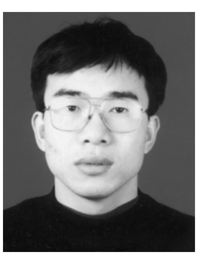

Hongliang Fang received the B.S. degree in geography from East China Normal University, Shanghai, China, in 1993, the M.S. degree in cartography and GIS from the Institute of Geography, Chinese Academy of Sciences, Beijing, China, in 1996, and the Ph.D. degree in remote sensing from the University of Maryland, College Park, in 2003.

He is currently a Research Associate (Post-Doc) with the Department of Geography, University of Maryland. He is interested in land surface data assimilation, land surface parameter retrieval from remotely sensed data, as well as biomass and environmental monitoring. His current research activities mainly involve producing quality land surface products, satellite data products validation, and applying remote sensing data in modeling of the agricultural systems. In his native country China, he has conducted research in two areas: one is about the sustainable development of the Yellow River Delta, while the other is about rice crop production estimation in China.

Shunlin Liang (M'94–SM'00) received the Ph.D. degree in remote sensing and GIS from Boston University, Boston, MA.

He was a Postdoctoral Research Associate at Boston University from 1992 to 1993, and a Validation Scientist of the NOAA/NASA Pathfinder AVHRR Land Project from 1993 to 1994. He is currently an Associate Professor at the University of Maryland, College Park. His present research interests focus on land surface data assimilation and quantitative optical remote sensing. He is a member of NASA ASTER, MISR, and MODIS science teams and coedited a special issue of *Remote Sensing Reviews*.

Dr. Liang organized the International Forum on BRDF at San Francisco, CA, in December 1998. He has chaired various sessions of international conferences and served as Chairman of the IEEE Geoscience and Remote Sensing Society, Washington/North Virginia Chapter (2000). He is Co-Chairman of the International Society for Photogrammetry and Remote Sensing Commission VII/I Working Group on Fundamental Physics and Modeling. He is an Associate Editor of the IEEE TRANSACTIONS ON GEOSCIENCE AND REMOTE SENSING.

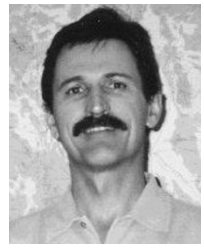

Mitchel P. McClaran received the B.Sc. degree in conservation of natural resources, the M.Sc. degree in range managemen, and the Ph.D. degree in wildland resources sciences, in 1979, 1981, and 1986, respectively, all from the University of California, Berkeley.

In 1986, he joined the faculty in the School of Natural Resources, University of Arizona, Tucson, and in 2001, was promoted to Professor of range management. Since 1990, he has developed a research program studying the long-term vegetation changes on the Santa Rita Experimental Range in southern Arizona.

Willem J. D. van Leeuwen received the B.Sc. and M.Sc. degrees in soil science from the Agricultural University in Wageningen, Wageningen, The Netherlands, in 1985 and 1987, respectively, and the Ph.D. degree in soil and remote sensing science from the University of Arizona, Tucson, in 1995.

He has been a Research Scientist and an active member of the MODIS land science team since 1996 and is an Adjunct MODIS team member since 2000. From 1999 until 2002, he was a Research Scientist with Météo France, Toulouse, and worked on a European Community project that involved polar and geostationary satellites and albedo algorithm development. He is currently a Research Scientist in the Office of Arid Lands Studies, Arizona Remote Sensing Center, Tucson, working on ecological applications using remote sensing technology and is involved in web-based decision support tool development for natural resource management (RangeView): *http://rangeview.arizona.edu*. His main research interests revolve around decision support Ssystems and the integration of remotely sensed products in geographic information sSystems in order to monitor natural resources and vegetation dynamics through time and across landscapes.

Sam Drake, photograph and biography not available at the time of publication.

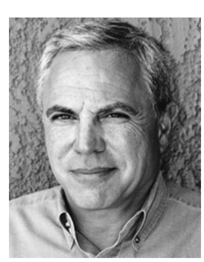

Stuart E. Marsh received the B.S. degree in geology from George Washington University, Washington, DC, the M.S. and Ph.D. degrees in applied earth sciences from Stanford University, Stanford, CA, in 1973, 1975, and 1979, respectively.

He is currently Professor and Chair of the Arid Lands Resource Sciences Interdisciplinary Ph.D. Program and Director of the Arizona Remote Sensing Center, University of Arizona, Tucson. He also holds a joint faculty appointment with the Department of Geography and Regional Development. He is currently involved in a broad range of research designed to assess surface environmental conditions utilizing advanced remote sensing and geographic information system technologies. These research efforts have attempted to enhance our abilities to employ these technologies to address problems concerning land use and land cover change and environmental hazards. He is the author of numerous publications concerning the application of remote sensing and geographic information science to environmental problems.

Allison M. Thomson received the B.A. degree from Carleton College, Northfield, MN, and the M.S. degree in environmental management from Duke University, Durham, NC, in 1997 and 1999, respectively.

She is currently a Research Scientist with the Joint Global Change Research Institute, a collaboration between the Pacific Northwest National Laboratory and the University of Maryland, College Park. Her current research activities focus on simulation modeling of the impacts of climate variability and change on agricultural systems. Recent projects examine the potential role of soil carbon sequestration as a mitigation strategy for anthropogenic climate change in the United States and China, and the role of historical management on soil carbon in arid rangelands.

Ms. Thomson was awarded the American Water Resources Association's Boggess Award for best paper published in the *Journal of the American Water Resources Association* in 2003.

Roberto Cesar Izaurralde received the B.Sc. degree in agronomy from Universidad Nacional de Cordoba, Cordoba, Argentina, in 1972, and the M.Sc and Ph.D degrees in soil science from Kansas State University, Manhattan, in 1981 and 1985, resectively.

He is currently a Laboratory Fellow with the Joint Global Change Research Institute (a collaboration of the Pacific Northwest National Laboratory (PNNL) and the University of Maryland). His current research focuses in the areas of modeling 1) the impacts of climate change and variability on terrestrial ecosystems and water resources and 2) carbon sequestration in and greenhouse gas emissions from agricultural soils. Before joining PNNL in 1997, he served as Chair of Resource Conservation in the Department of Renewable Resources, University of Alberta. In his native country Argentina, he studied at and later joined the Facultad de Ciencias Agropecuarias, Universidad Nacional de Cordoba. He was an Invited Professor with the Universidad Nacional de Cordoba in 1996 and 1999 and with the Universidad Catolica de Cordoba in 1977 to 1980.

Dr. Izaurralde received the American Water Resources Association's Boggess Award for best paper published in the *Journal of the American Water Resources Association* in 2003, two PNNL Outstanding Performance Awards in 1999 and 2002, and a Fulbright Fellowship, 1980–1981. He is a member of the Soil Science Society of America, the American Society of Agronomy, and the American Association for the Advancement of Science.

Norman J. Rosenberg received degrees in soil science and meteorology from Michigan State University, East Lansing, Oklahoma State University, Stillwater, and Rutgers University, Piscatway, NJ.

He currently leads research on the impacts of climatic variability and potential change on water resources, agriculture, and unmanaged ecosystems at Battelle's Pacific Northwest National Laboratory (PNNL), Joint Global Change Research Institute (JGCRI), University of Maryland, College Park. Also, under JGCRI's Global Technology Strategy Program (GTSP), he is responsible for efforts to develop an understanding of the potential role of biotechnology and genetic engineering in mitigation of global climatic change. Since joining Battelle in 1992, he has coordinated research that provides information to JGCRI's Global Change Assessment Model and has integrated assessment tools for understanding the causes and potential effects of environmental change, means of mitigation, and adaptation to change that is unavoidable. As one means of mitigation, he has conducted research on sequestration of carbon in agricultural soils. He was Principal Organizer of a workshop and other efforts that led to creation of the DOE-sponsored multilaboratory research program Carbon Sequestration in Terrestrial Ecosystems. Prior to joining PNNL, he was Director of the Climate Resources Program, Resources for the Future (RFF), Washington, DC. Before joining RFF in 1987, he was George Holmes Professor of Agricultural Meteorology with the University of Nebraska, Lincoln, which he joined as an Assistant Professor in 1961. He is Associate Editor of the journals *Climatic Change* and *Agricultural and Forest Meteorology*.

Dr. Rosenberg is a Fellow of the American Society of Agronomy, the American Meteorological Society, and the American Association for the Advancement of Science.